academicJournals

Vol. 10(15), pp. 436-455, 16 August, 2015
DOI: 10.5897/IJPS2015.4296
Article Number: F0F4B9E54538
ISSN 1992 - 1950

http://www.academicjournals.org/IJPS

International Journal of Physical Sciences

Full Length Research Paper

Electrical conductivity and uniaxial shear tests on soil samples

Tekin Yeken

Department of Technical Programs, İ. Uzunyol Vocational School, Kocaeli University, TR41800 Hereke/Kocaeli, Turkey.

Received 22 March, 2015; Accepted 13 July, 2015

Soil properties should be well known for the earthquake-resistant structural design studies and other engineering researches. It is aimed to understand the region's soil-structure properties as a result of the practices carried out to determine the mechanical properties and elastic-dynamic character of the units under load. Accordingly, considering the factors that affect the physical and mechanical properties such as mineralogical and petrographic structures, water content, porosity-permeability, chemical composition, texture, and clay-mineral content of the rocks play an important role. Therefore, the data regarding the load-bearing capacity of the ground, seismicity and active tectonics are required for analyzing the study area. In this study, mechanical loading-shear and electrical-resistivity tests were applied simultaneously to the soil samples taken from a seismo-active area in Kocaeli to determine the relationship between these properties. Determination of the electrical resistivity response during the deformation of the material constituted the purpose of this experimental study. Elastic-dynamic parameters were investigated using the relative relationships in terms of physical and mechanical parameters in order to understand the behavior of the sample. The result of experimental study indicated that current increased linearly with the stress before deformation. Similar relationships have been observed for the self-potential parameters and stress. In experiments; sample rate is defined as the axial length of the 1.5 to 2.0% contraction critical threshold. This proportional relationship can be considered in earthquake prediction observation.

Key words: Soil investigation, electrical resistivity, potential difference, uniaxial stress, conductivity, deformation.

INTRODUCTION

Depending on the developing geological technology, several geotechnical applications and laboratory studies have been carried out in order to obtain detailed information on the loading and mechanics of soil (Brace and Orange, 1968; Jaeger and Cook, 1969; Roylance, 2001; Bieniawski, 1992; Bieniawski and Denkhaus, 1994). In such studies, it was aimed to determine the behaviors of the units constituting the soil under loading as well as the physical and mechanical properties of them. To this end, determination of the elastic-dynamic parameters of the soil is important in terms of the structure-soil relationship.

It is known that rocks under stress are deformed depending on the dynamic properties of the ground and

E-mail: tyeken@yahoo.com

its active tectonic effect. As a result of this stress, significant changes occur in the electro-chemical activities and other physical properties of rocks (Brace, 1971; Wawersik and Brace, 1971; Shon, 1998; Clint, 1999). The conductivity of the layers in the ground is determined with the particles forming the layer and the electrical current conductivity capacity of the solution between these particles. Especially, the salinity in the solution and the ambient temperature affect conductivity (Starfield and Fairhurst, 1968; Nasuf, 1977; Idziak and Stan-Kleczek, 2006). The size of the particles forming the units, the clay content, porosity-permeability and other physical properties of them as well as their loading under pressure are also factors affecting electrical conductivity.

Noticeable changes are observed in the resistivity and potential difference values of the units before and after brittle fracture. Changes which occur in the electromagnetic and other geochemical parameters in a soil layer can be observed periodically. In the study of Brace and Orange (1968), considered one of the first experimental studies on the issue, the electrical resistivities of water-saturated crystalline rocks under the effect of pressure were experimentally correlated. On the other hand, Brace (1971) examined the electrical resistivities of the rock samples during the fracture. Kate and Gokhale (1998) and Kate and Rao (1989) determined the electrical conductivity behaviors of sandstones subjected to uniaxial compression. In a similar study, Idziak and Stan-Kleczek (2006) determined the physico-mechanical properties of volcanic rock samples and functional relationships of their electrical resistivities experientially.

Deformation of the pre-established static equilibrium with the effect of the additional loading transferred to the ground and regeneration of it is in conformity with the power distribution principle of physics. However, any changes in the mechanical properties of the rocks exposed to deformation due to pressure and stress also occur in their physical properties (Main et al., 1990; Clint, 1999; Kahraman and Yeken, 2008). The bonds between the unit size particles and the relative relationships between the tissues vary depending on the loading and dynamics relationships.

Geological units with high density and no fractures or clay content also usually have high electrical conductivities. As a result of the seismic refraction applications, the layers having these properties were determined to have high seismic velocities as well. On the other hand, rocks containing clay to a certain extent give low resistivity response depending on the amount of the clay. With the physical and mechanical tests implemented for the soil samples taken from any region, important data on the soil dynamics and statics are obtained. In this case, their electrical conductivity varies depending on the clay content and porosity. The purpose of this study is to observe the response of the electrical conductivities on uniaxial shear loading of the ground sample.

In this laboratory work, simultaneously with the electrical parameters of mechanical stress effects were examined. The purpose of this study is the measurement of the electrical parameters in response to pre-deformation of the material.

METHODS

Compressional-resistance and electrical conductivity tests were simultaneously applied to the cylindrical samples 50 mm in diameter and 100 mm in height (Figure 1a and b). The samples were divided into three equal parts and copper plates were placed between them in order to provide convenience in theoretical calculations. In the apparatus, the center sections were used for potential difference electrodes and the other connections for current electrodes. Disturbed and undisturbed samples were taken from the field and prepared for the application. The samples were subjected to uniaxial loading at different levels. With the deformation and disturbance occurring as a result of the compressional loading, their self-potential (SP) and electrical current-resistivity response were numerically determined (Figure 2).

In case of diametrical deformation (ε_d) and axial unit deformation (ε_a), the values are read from the data scale and recorded in each load increase.

ℓ_0 = Initial length of the sample, $\Delta\ell$ = When the change in the length of the sample is taken;

Axial unit deformation (ε_a), $\varepsilon_a = \frac{\Delta\ell}{\ell_0}$

Electrical resistivity

In the general sense, it is defined as the measurement of the potential distribution of the electric field in the ground generated by the electric current transferred into the ground. Determination of the potential value at a distance of (*l*), at a given point in a homogeneous and isotropic medium constitutes the purpose of the resistivity method. A homogeneous medium was chosen in order to ground the method on a more simple and basic mathematical basis. Resistance of a circuit is expressed as follows according to Ohm's law;

$R = \Delta V / \Delta I \quad (\Omega)$

However, the resistance for an element with L dimension and V_A cross-section is expressed as follows (Figure 3):

$R = \rho L / A$

The following expression is obtained from here;

$\Delta V / \Delta I = \rho . L / A$

$\Delta V = \rho . \Delta I . L / A$

ΔV: Potential difference (mV), ρ: Resistivity (Ohm-m), ΔI: Current (mA), L: Length (m), A: Cross section (m^2), G:Geo. Constant,

$-\int dV = \rho I \int dr / ds$

$-V = \rho I / 4\pi \int dr / r^2$

Due to the semi-infinite surface, the following expressions are obtained;

$\Delta V = \rho . I / 2\pi \, 1/r$

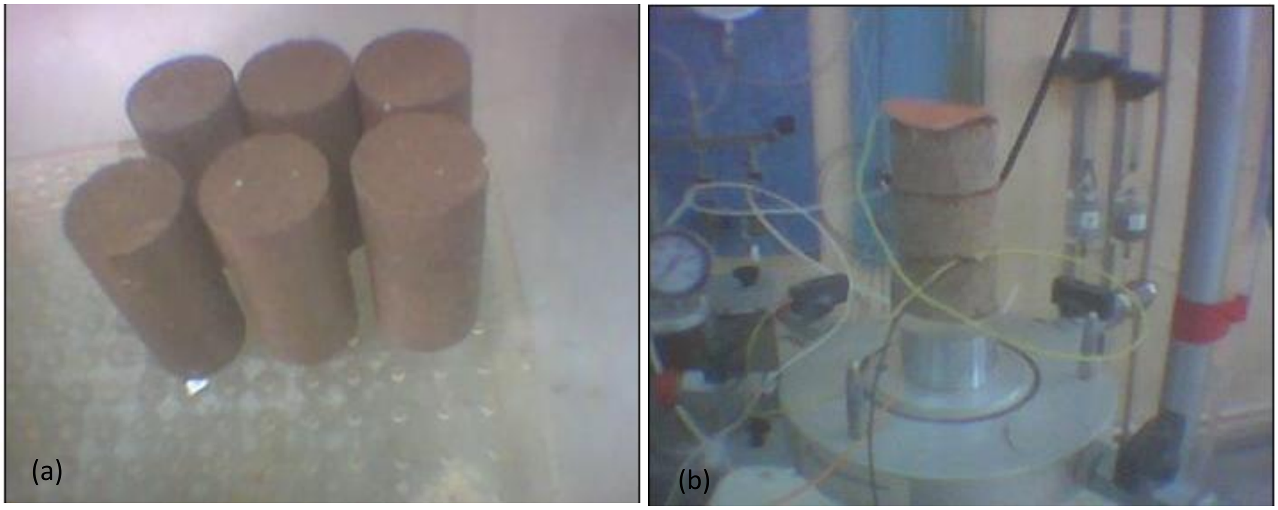

Figure 1. (a) Soil sample, (b) Uniaxial shear test and electrical measurement apparatus.

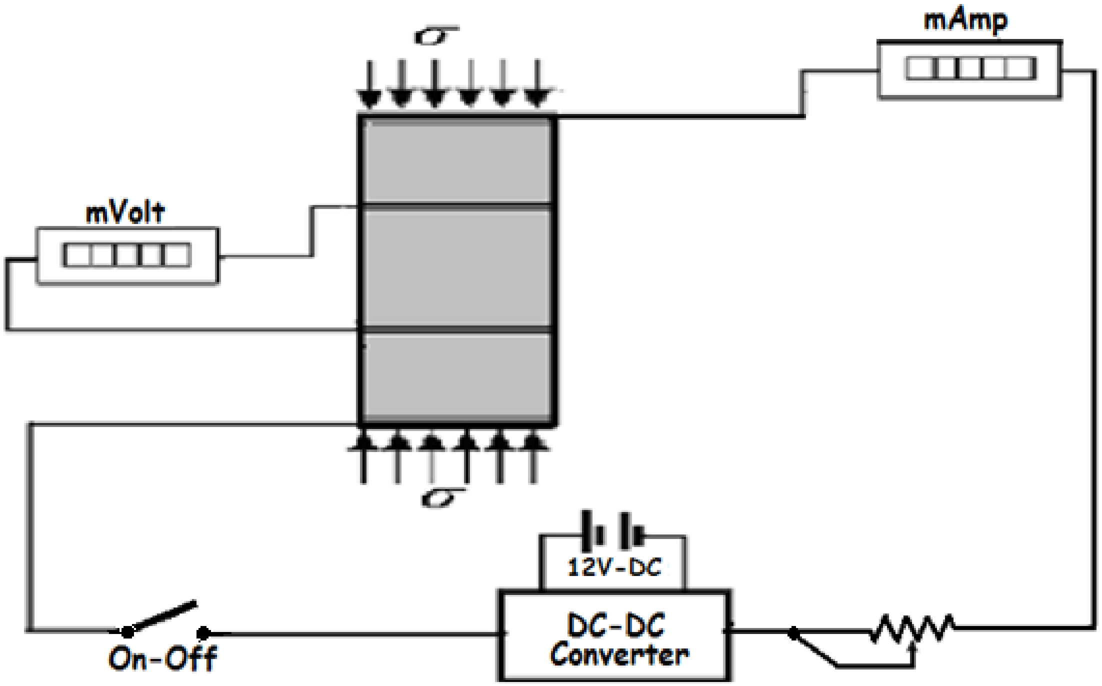

Figure 2. Mechanical and electrical test diagram.

Resistivity from generalized equation;

$\rho = G. (\Delta V / I)$ (Ωm)

Potential difference

In the implementation, uniaxial stress and its consequential natural potential relationship were measured. It is based on the basis of the potential difference change depending upon the amount of the pressure. The differences in the physical properties of the samples cause potential difference change. In natural environment, there are secondary potentials which occur as a result of the electrochemical reactions such as vegetation potential arising from bioelectrical activities and diffusion potential caused by liquid flows in the earth. However, galvanic potentials which occurred as a result of the concentration differences between the particles were measured for the samples used in the experiment. Uniaxial shear and resistance tests were applied to the samples and potential difference changes of the material were examined during the deformation period

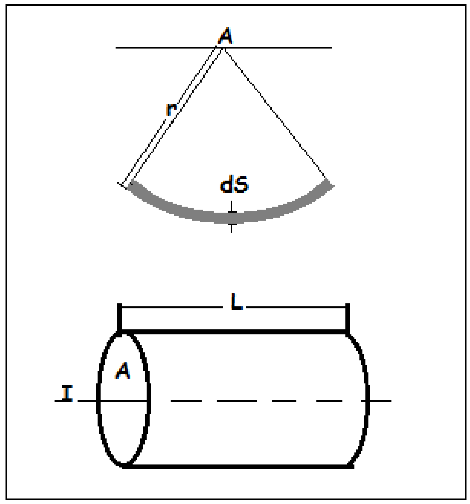

Figure 3. Resistivity of an element with unit size and unit area.

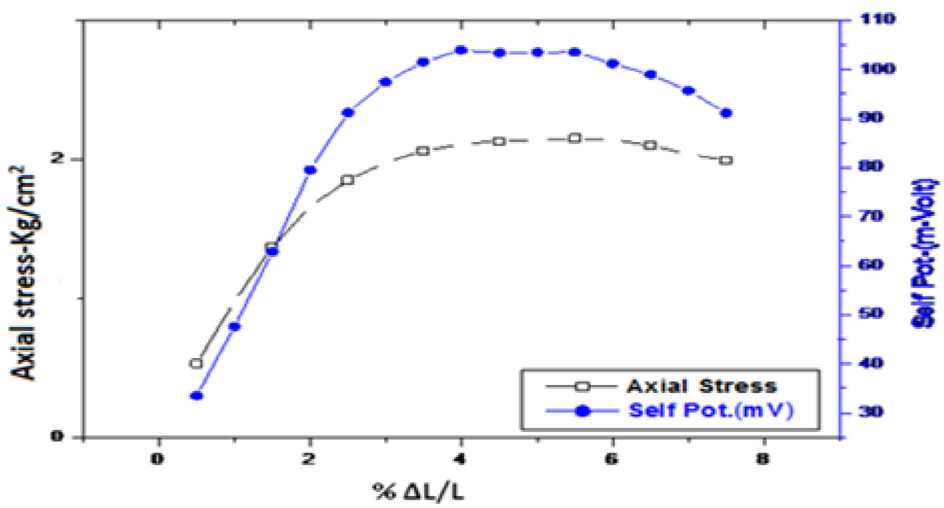

Figure 4. Potential difference changes versus axial stress. (Sample:A-01).

(Figures 4 to 13).

EVALUATION

In monitoring the changes in the electrical and mechanic parameters in these studies, petro-physical property of the environment is taken into consideration in especially fine-grained soils. In the determination of seismic "gap" areas and risk-bearing regions, the prediction modellings to be applied are important. In especially prediction modelling studies, the self-potential values and resistivity relationship of the fine-grained clayey-silty layer can be monitored more specifically than rock units with high mechanical endurance. On the other hand, monitoring the parameters for prediction in pre-earthquake period (foreshock) can provide important nonnumeric cues about critical anomaly and energy discharge as a result of brittle fracture.

In the study, the soil samples analyzed under uniaxial stress were examined in disturbed and undisturbed forms. Electrical resistivity and current-potential difference behaviors of the disturbed samples under axial stress were correlated (Figures 4 to 13). In Figures 4, 5 and 6; potential difference responses depending on the applied axial stress were determined. A curvilinear cohesion is observed until the material deformation limit. However, SP values tend to decrease sharply with the

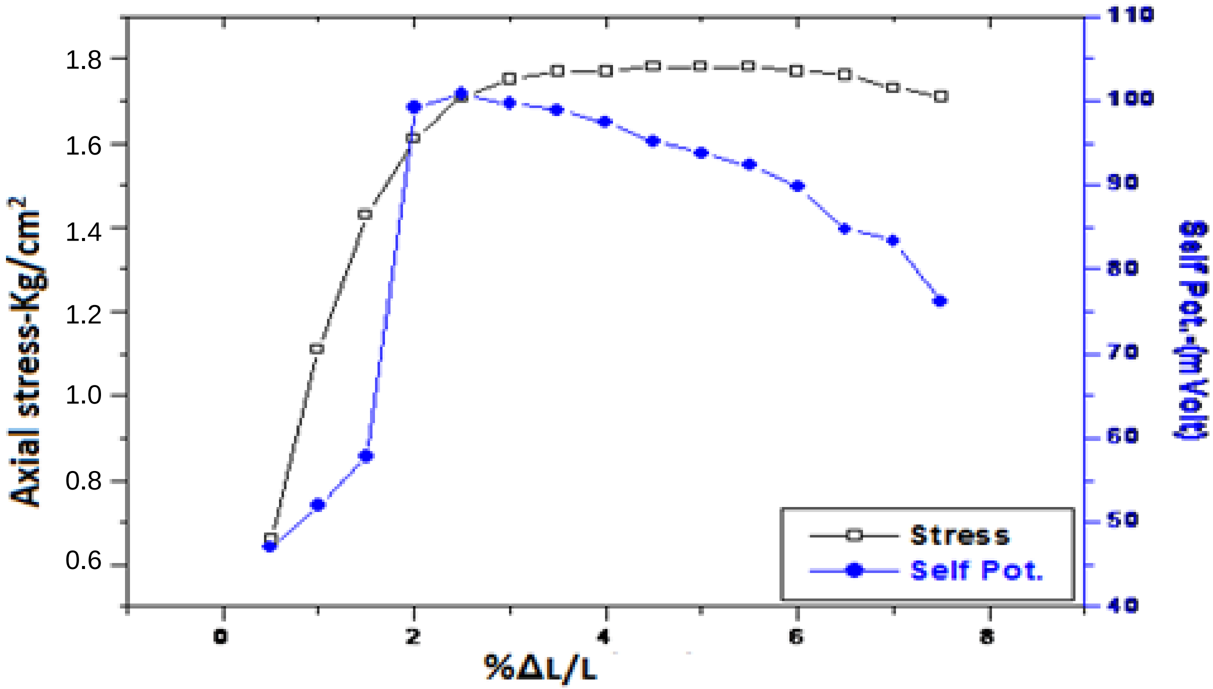

Figure 5. Potential difference changes due to the axial stress. (Sample:A-02).

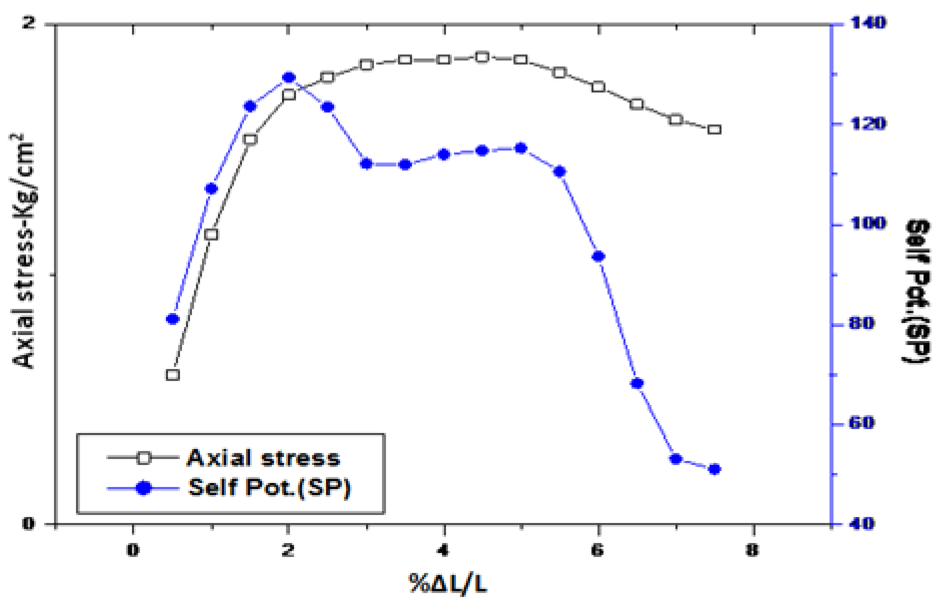

Figure 6. Potential difference changes due to the axial stress. (Sample:A-03).

increase in the fractured medium as a result of the loading dependent on the swelling of the material. In Figure 7, the relationship between the axial stress and resistivity was analyzed. As the elastic material was compressed with pressure, the electrical resistivity values decreased in an inverse proportion. In Figures 8 and 9, the change in the current given to the circuit under compressive stress was specified. For both samples, post-deformation current behaviors are compatible. In Figure 10, the functional relationship between the current given to the material and the inversely proportional change in the potential difference is compatible according

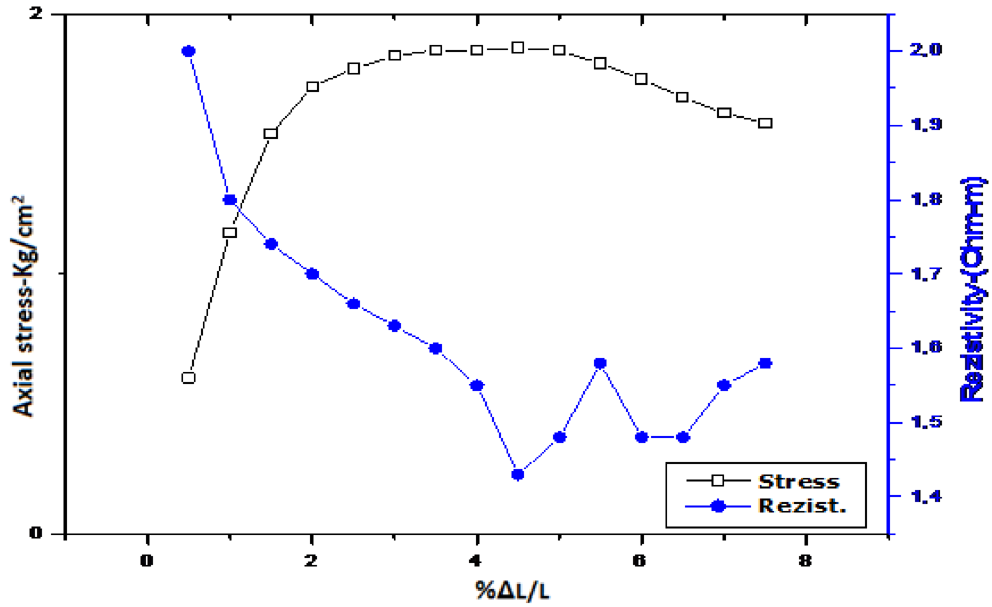

Figure 7. Resistivity versus axial stress (Sample:A-04).

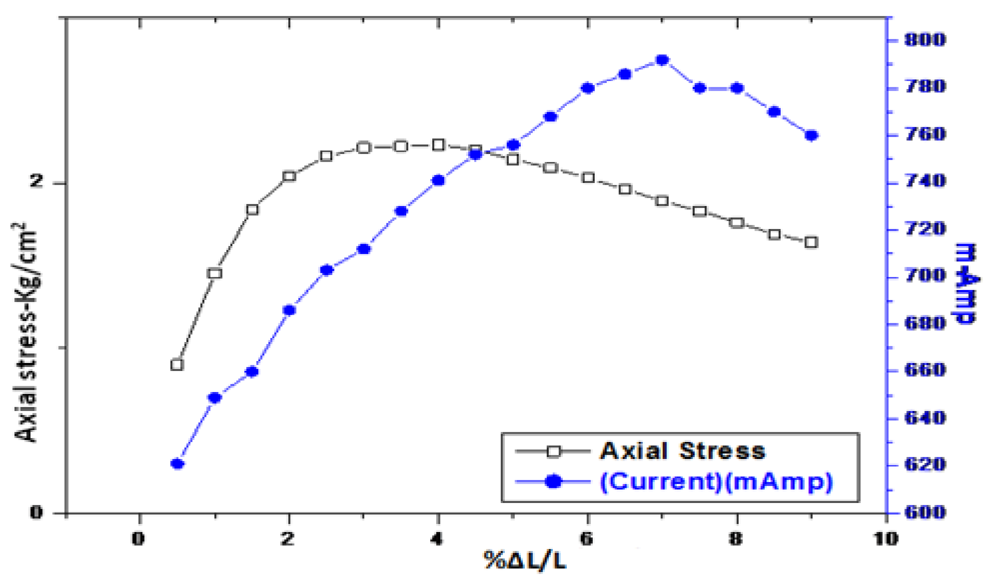

Figure 8. Current versus axial stress (Sample:A-05).

to the Ohm principle and theory. In Figures 11 and 12, the SP relationships of the undisturbed samples (UD) under axial stress were determined. In Figure 13, the current, stress and proportional relationships in case of longitudinal construction (%DL/L) were determined.

DISCUSSION AND CONCLUSION

The following findings were obtained according to the studies carried out:

(i) Determination of the responses of electrical parameters to be created for the medium with the effect of loading in a soil sample with high activity constituted the purpose of this study.
(ii) In this experimental study, a uniaxial construction at a rate of approximately 1.5 to 2.0% was observed in the length of the material with a linear loading in fine-grained soils. On the other hand, an increase was observed in the

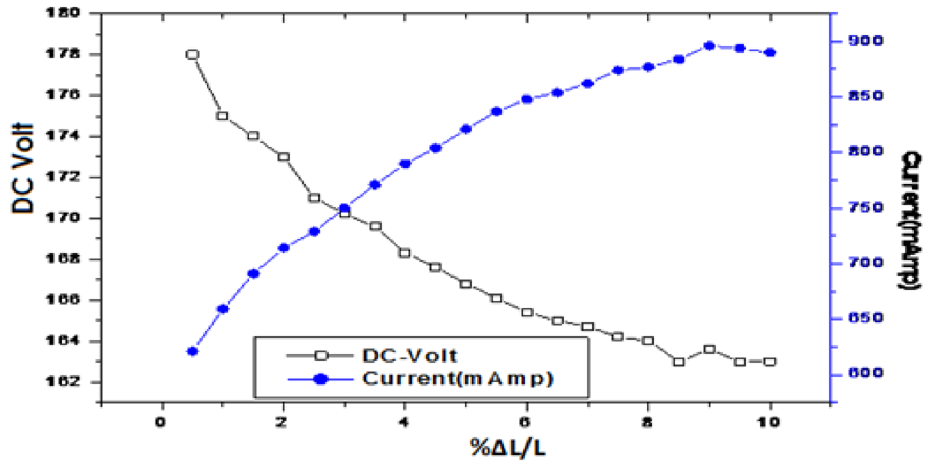

Figure 9. Current versus DC voltage (Sample:A-07).

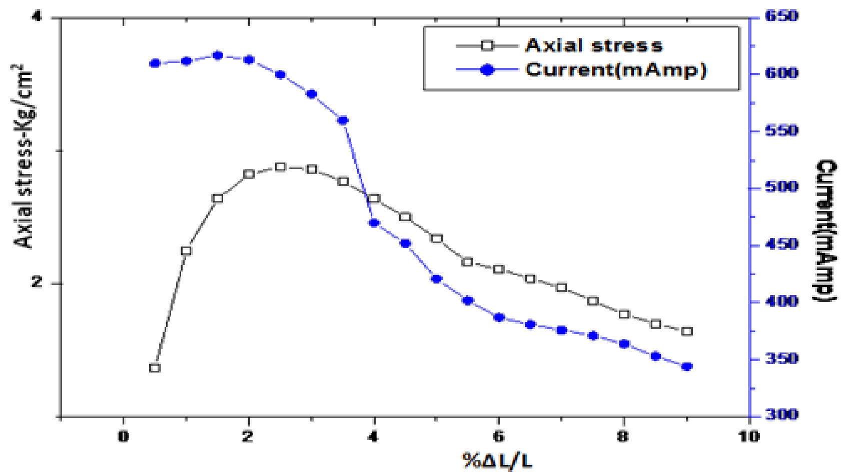

Figure 10. Current versus axial stress (Sample: A-10).

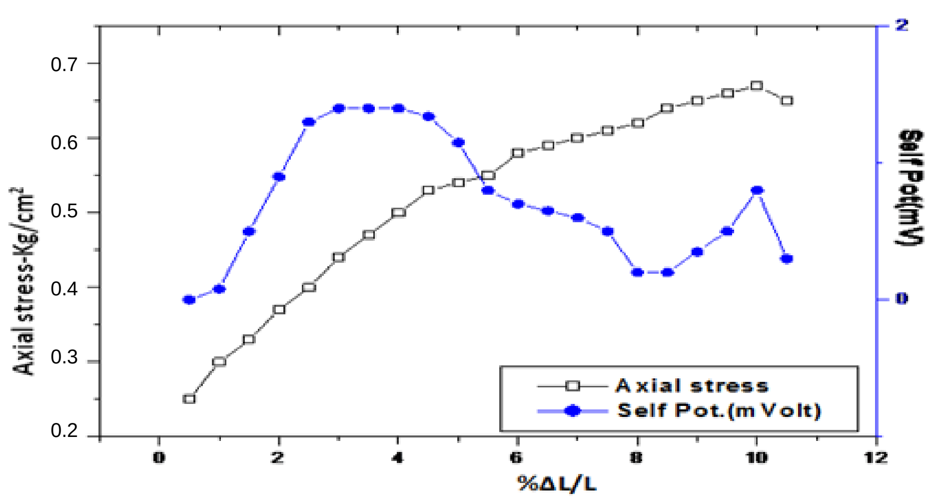

Figure 11. Self potential (SP) versus axial stress (A/UD-13).

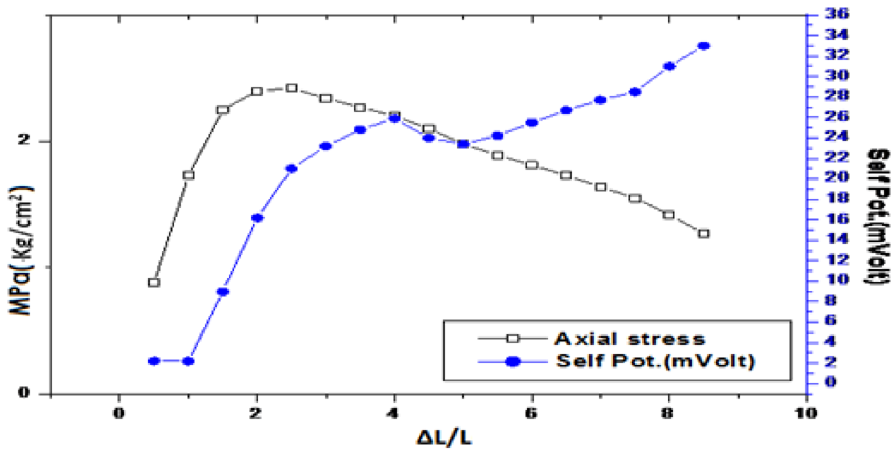

Figure 12. Self Potential (SP) versus axial stress (A-1/UD14).

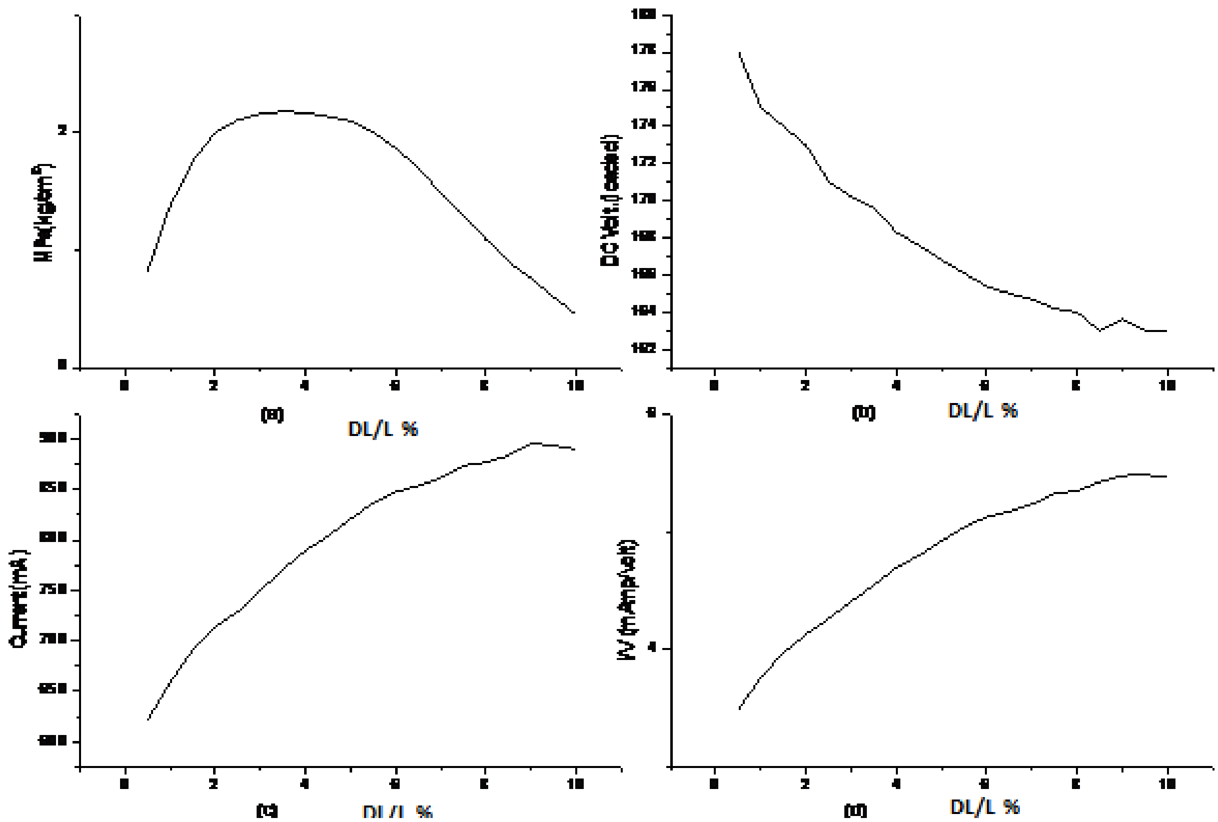

Figure 13. Axial stress, current and potential difference (A-1(07)). (a) Axial stress(Mpa), (b) DC voltage versus the circuit, (c) Current change (mA)versus ΔL/L %, (d) I(mA) / mV proportional change.

electrical conductivity until the fracture process of the material, whereas the conductivity values behaved erratically during the ductility or dispersion process of the material.

(iii) In the earthquake prediction studies, the periodic resistivity measurement technique correlated with the other electrical parameters is quite important. It is known that there will be increases in the resistivity values due to the pre-brittle fracture micro-tensile cavities in a rock under compressional stress. However, in response to the increase in pressure, there is an inversely proportional and sharp decrease in the resistivity values in a fine-grained compressed soil.

Conflict of Interest

The authors have not declared any conflict of interest.

ACKNOWLEDGEMENT

Author would like to thank the General Directorate of State Hydraulic Works (DSİ) – Department of Technical Research and Quality Control (TAKK) (Ankara), Soil Laboratory Branch Office and employees.

REFERENCES

Brace WF, Orange AS (1968). Electrical resistivity changes in saturated rocks during fracture and frictional siding: JGR 73(4):1433-1445.

Brace WF (1971). Resistivity of saturated crustal rocks to 40 km based on laboratory measurements; GG. Heacock, dd. the structure and Physical Properties of the Earth's Crust.: AGU, Washington, D.C. Geophys. Monog. Ser. P. 14.

Jaeger JC, Cook NGW (1969). Fundamentals of Rock Mechanics Methuen, LONDON.

Wawersik WR, Brace WF (1971). Postfailure behaviour of a granite and diabase. Rock Mech. 3:61-85.

Bieniawski ZT, Denkhaus HG (1994). Failure of fractured rock. Int. J. Rock. Mech. Mineci. 6(3):123-145.

Roylance D (2001). Introduction to Fracture Mechanics, Massachusetts Institute of Techn. Cambridge, MA. 02139.

Starfield AM, Fairhurst C (1968). How high-speed computers advance design of practical mine pillar system. Eng. Mining J. P.169.

Bieniawski ZT (1992). Design Methodology in Rock Engineering. ISBN-13:978-9054101215.

Nasuf SE (1977). A photo-elastic and Field investigation into the Interface problem in Rock Mechanics, Rhd thesis Univ. Strathclyde.

Idziak AF, Stan-Kleczek I (2006). Predicting the physico-mechanical properties of igneous rocks from electrical resistivity measurements, EUROCK 2006-Multiphysics Coupling and Long Term Behavior in Rock Mechanics, ISBN 0415410010, London.

Shon JH (1998). Physical properties of rocks: Fundementals and principles of petrophysics, Elsevier, Oxford. L P. 582.

Main IG, Meredith PG, Sammonds PR, Jones C (1990). Influence of fractal flaw distributions on rock deformation in the brittle field. In Deformation Mechanisms, Rheology and Tectonics, Knipe RJ, and Rutter EH, Geol. Soc. Lond. Special Publication. 54:81-96.

Kahraman S, Yeken T (2008). Determination of physical properties of carbonate rocks from P-wave velocity. Bull. Eng. Geol. Env. 67:277-281.

APPENDIX

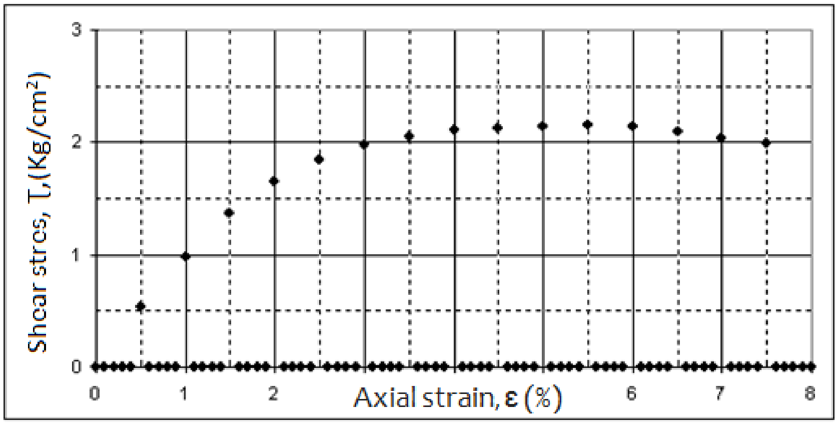

Sample no:A-1(01): **q_u** (kg/cm^2):2,15 **ΔL/L** (%):5,50.

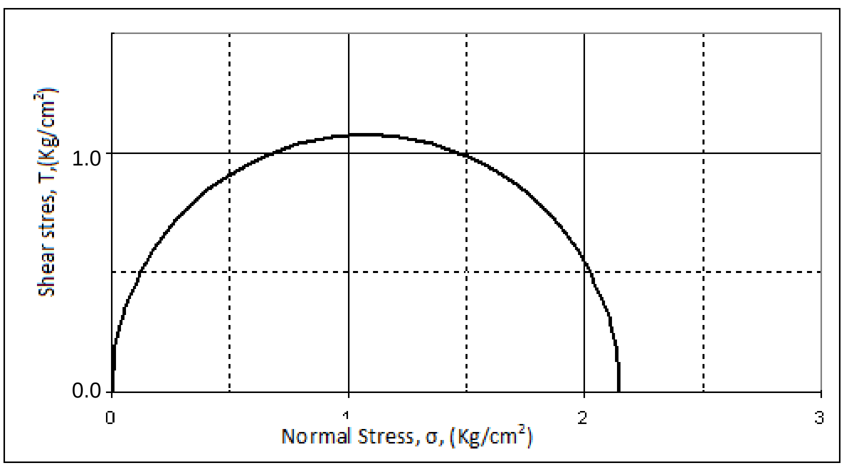

A (cm^2): 20,778 **F**(kg):44,6.

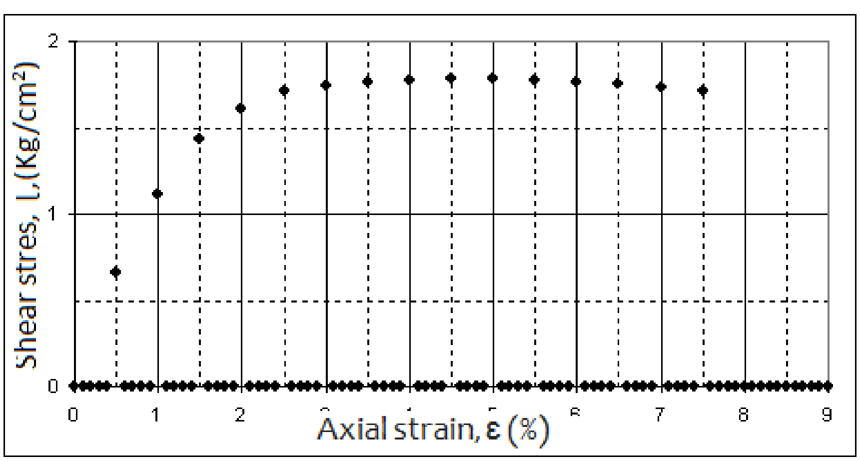

Sample no:A-1(02): **q_u** (kg/cm^2):1,78 **ΔL/L** (%):5,00.

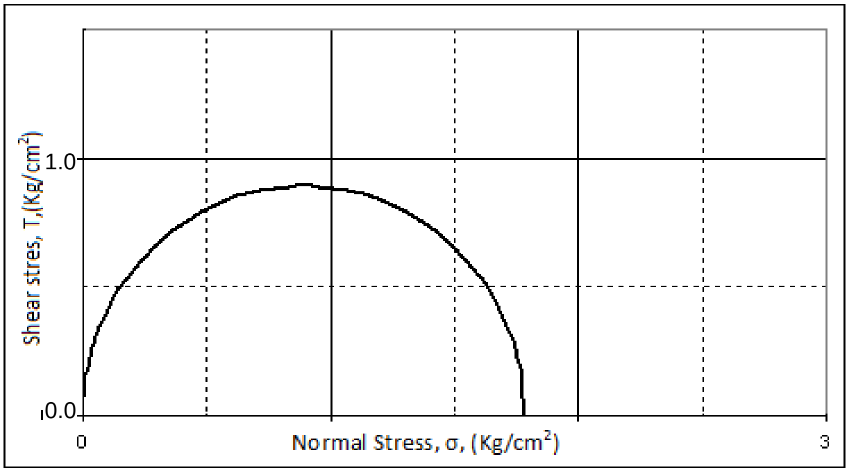

A (cm^2): 20,668 **F** (kg): 36,9.

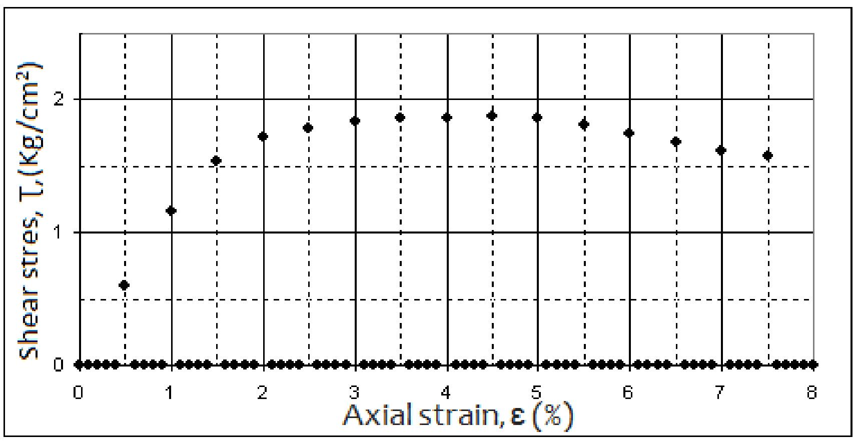

Sample no:A-1(03): **q_u** (kg/cm^2):1,87 **ΔL/L** (%):4,50.

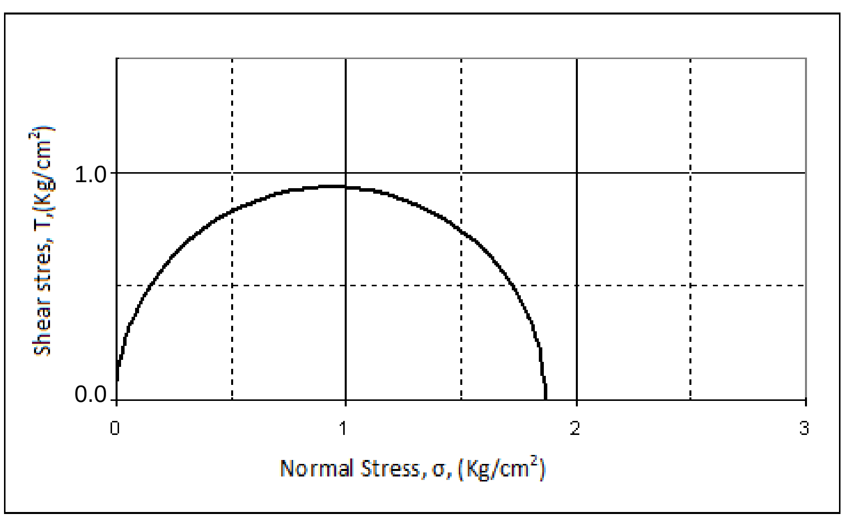

A (cm^2): 20,560 **F** (kg): 38,4.

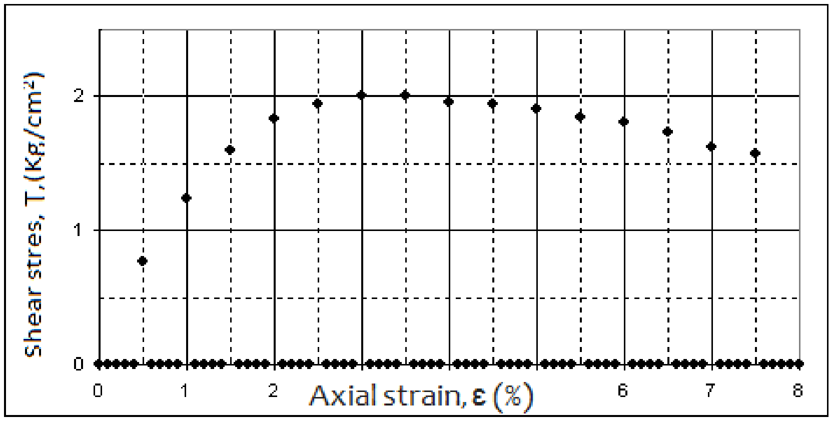

Sample no:A-1(04): q_u (kg/cm^2):2,01 **ΔL/L** (%):3,50.

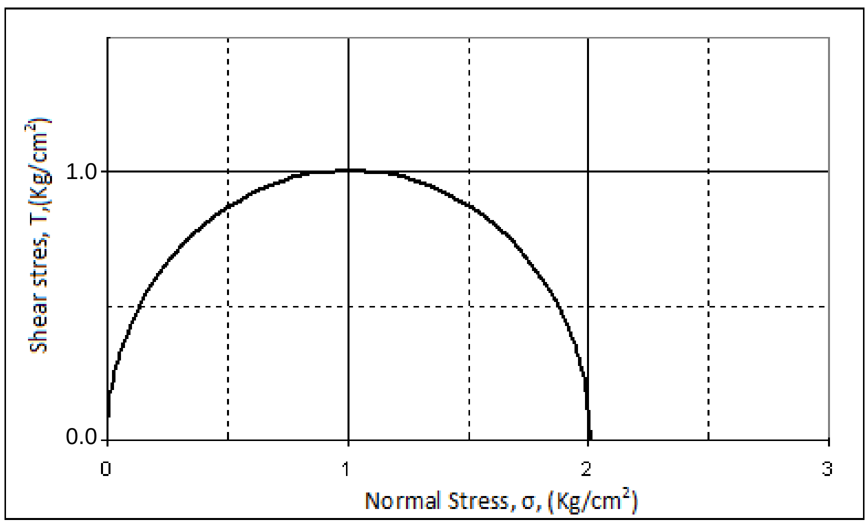

A (cm^2): 20,347 **F** (kg): 40,9.

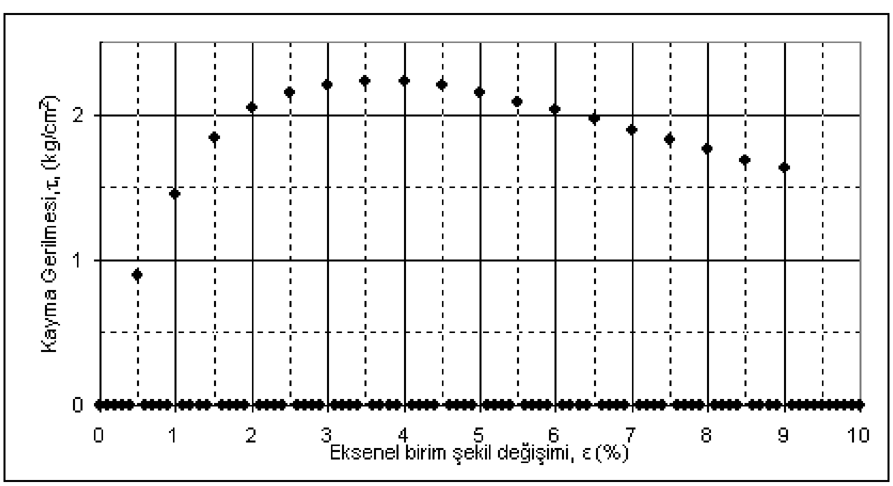

Sample no:A-1(05): q_u (kg/cm^2):2,23 **ΔL/L**(%):4,00.

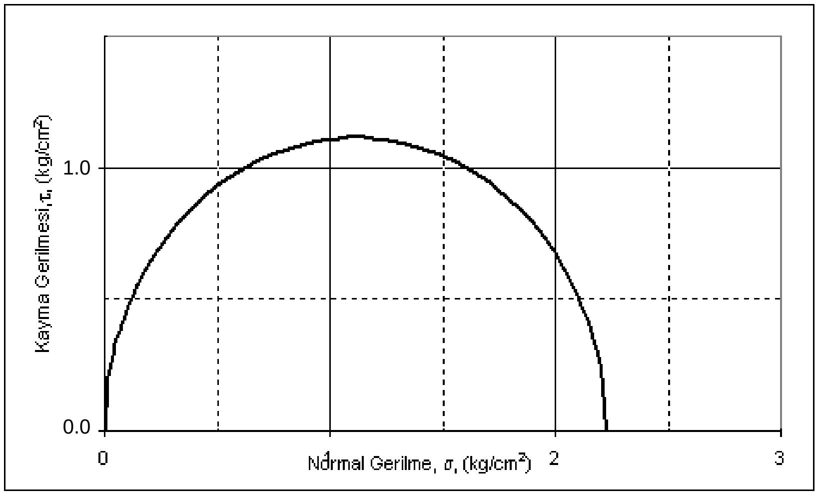

A (cm^2): 20,453 **F** (kg): 45,6.

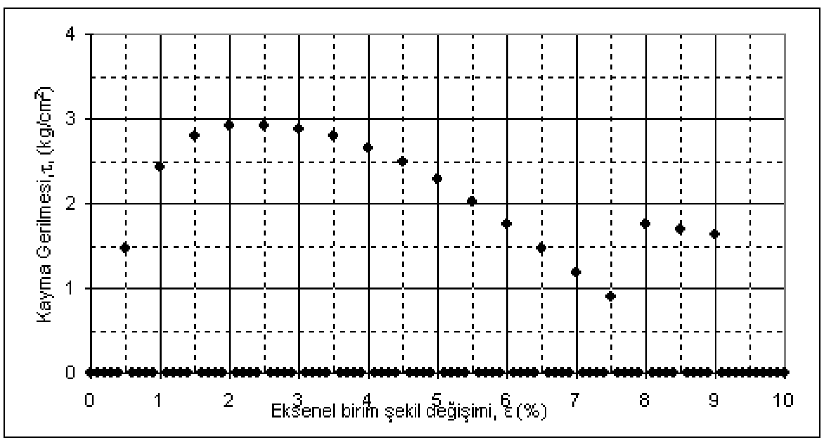

Sample no:A-1(06): $\mathbf{q_u}$ (kg/cm^2):2,92 **ΔL/L**(%):2,0.

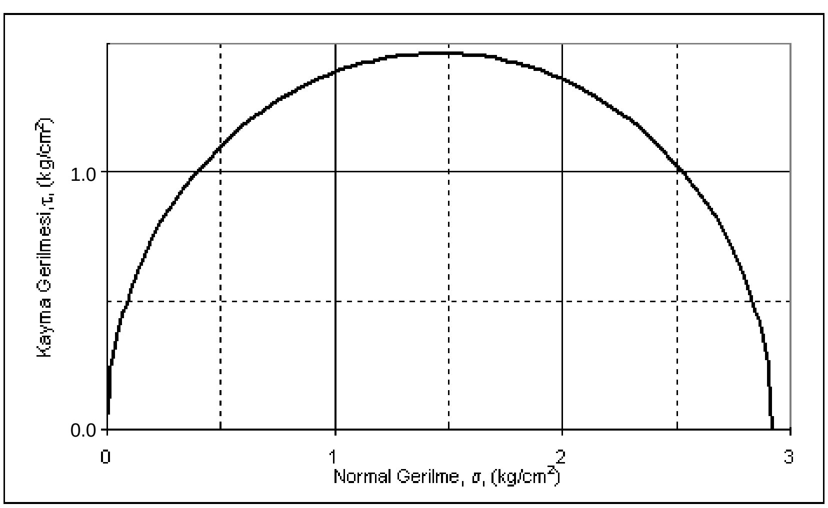

A (cm^2): 20,036 **F** (kg): 58,6.

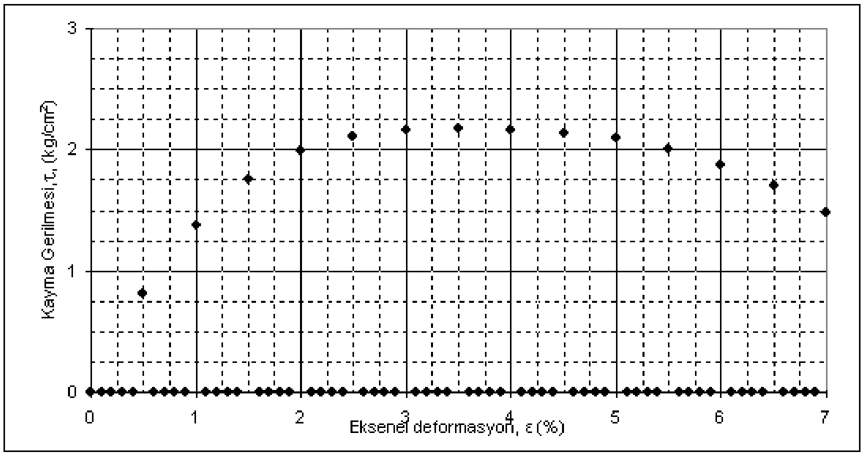

Sample no:A-1(07): $\mathbf{q_u}$ (kg/cm^2):2,18 **ΔL/L**(%):3,5.

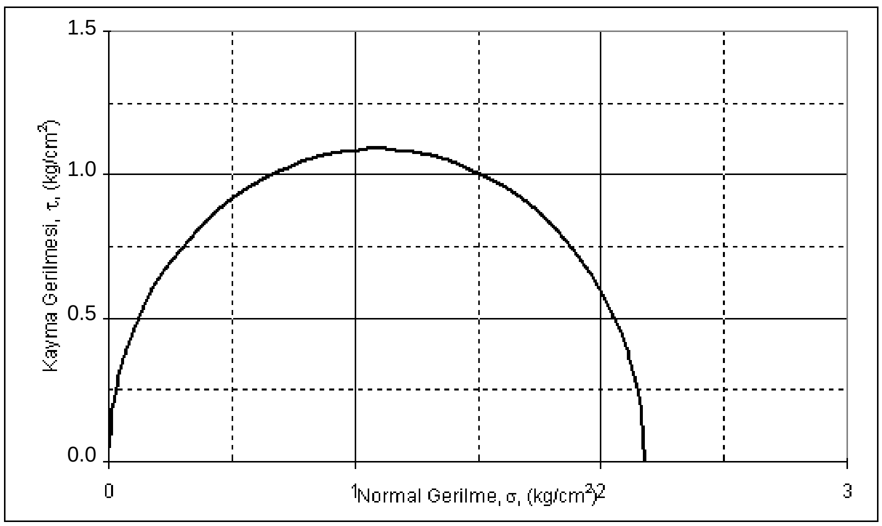

A (cm^2): 20,347 **F** (kg): 44,3.

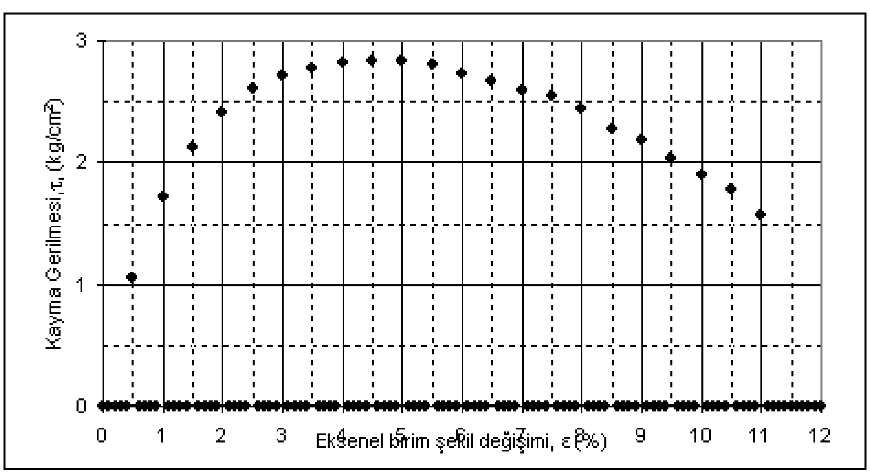

Sample no:A-1(08): $\mathbf{q_u}$ (kg/cm^2):2,83 **ΔL/L**(%):5,0.

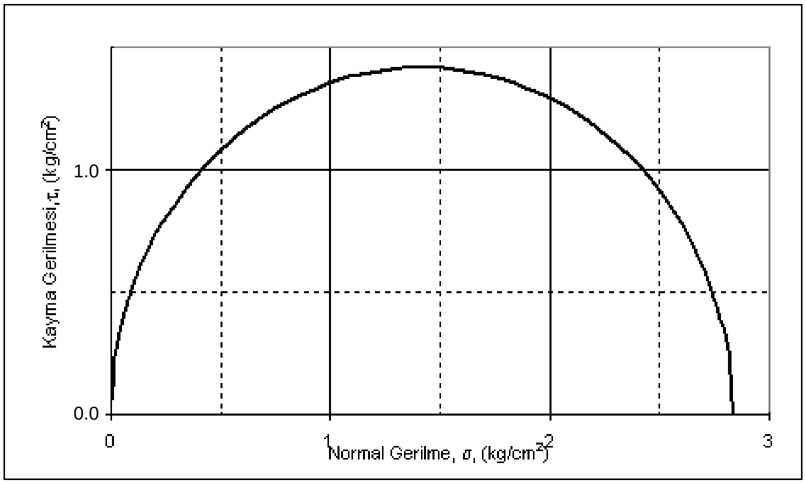

A (cm^2): 20,668 **F** (kg): 56,8.

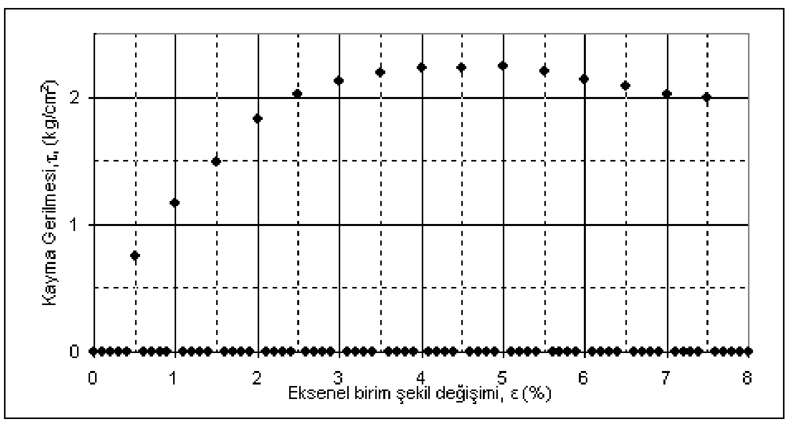

Sample no:A-1(09): $\mathbf{q_u}$ (kg/cm^2):2,23 **ΔL/L**(%):5,0.

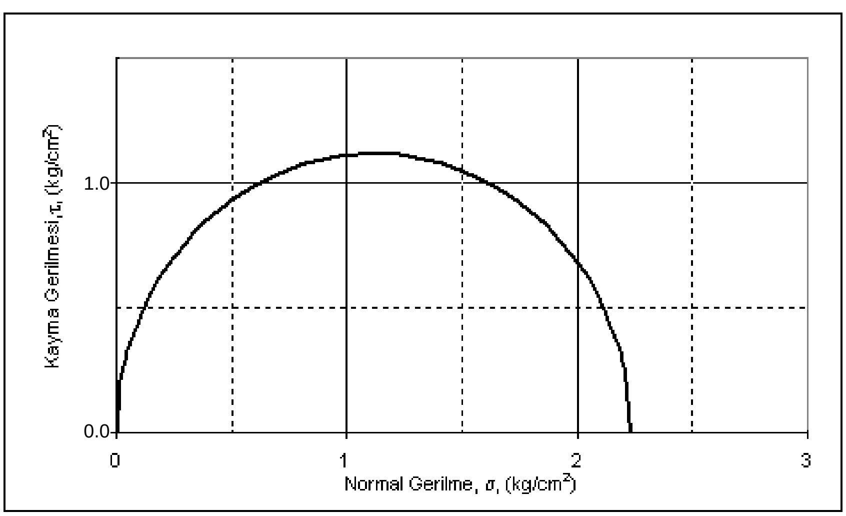

A (cm^2): 20,668 **F** (kg): 46,2.

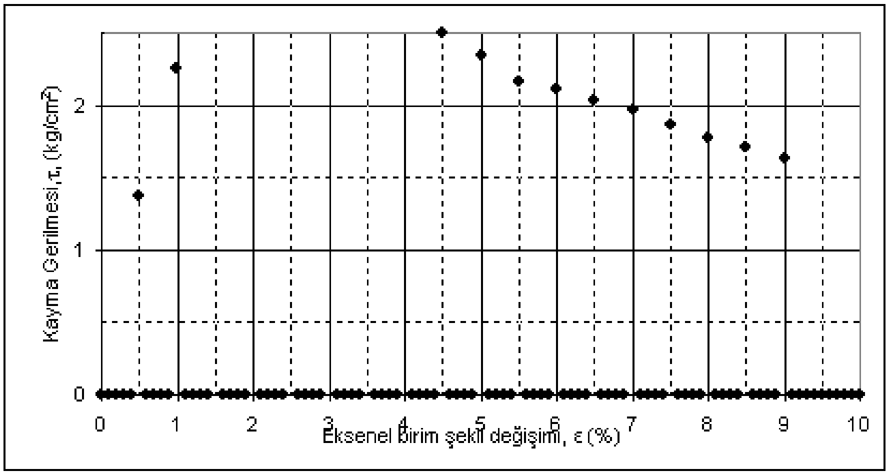

Sample no:A-1(10): **q_u** (kg/cm^2):2,88 **ΔL/L**(%):2,5.

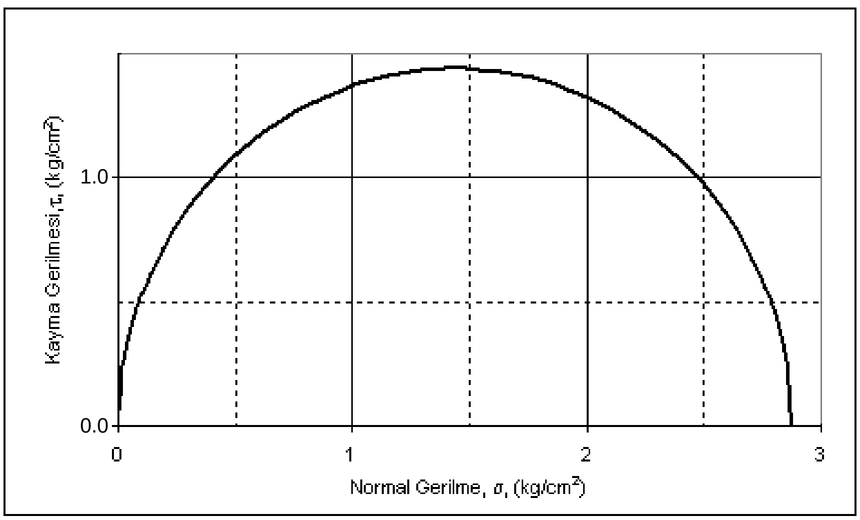

A (cm^2): 20,138 **F** (kg): 58,0.

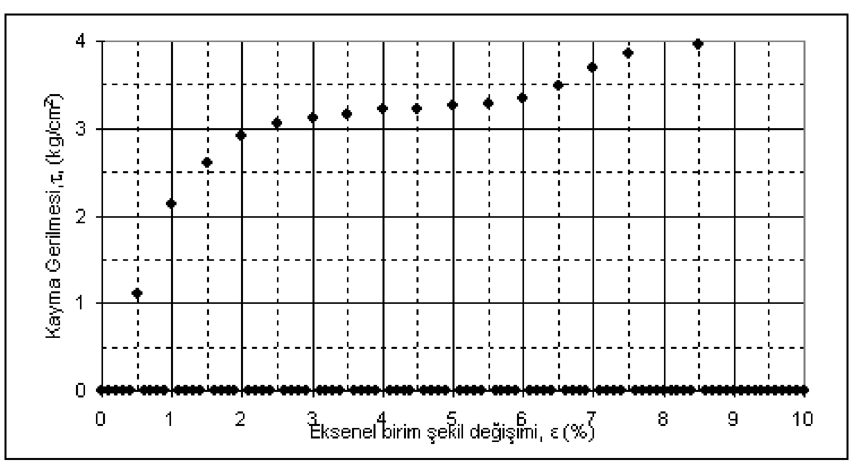

Sample no:A-1(11): **q_u** (kg/cm^2):3,96 **ΔL/L**(%):3,96.

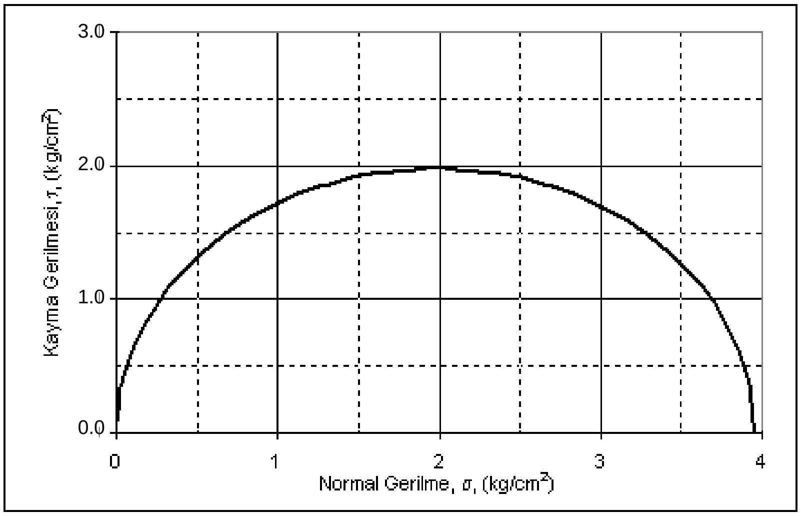

A (cm^2): 21,459 **F** (kg):84,9.

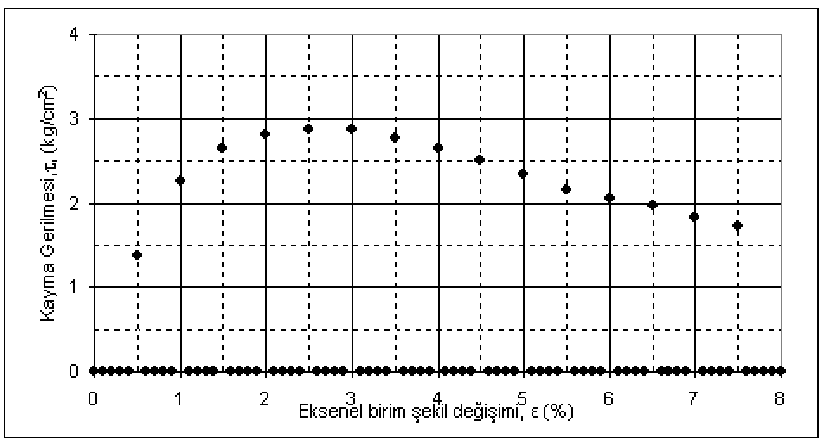

Sample no:A-1(12): **qu** (kg/cm^2):2,18 **ΔL/L**(%):4,9

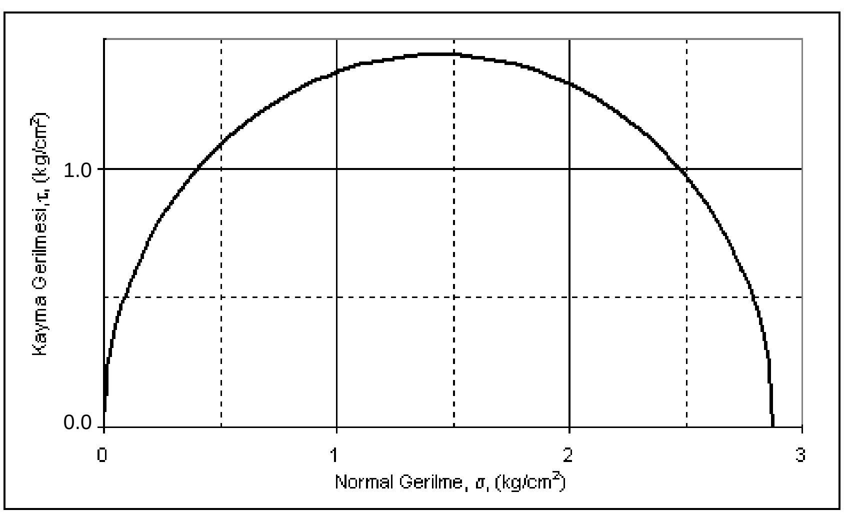

A (cm^2): 19,48 **F** (kg): 46,2.

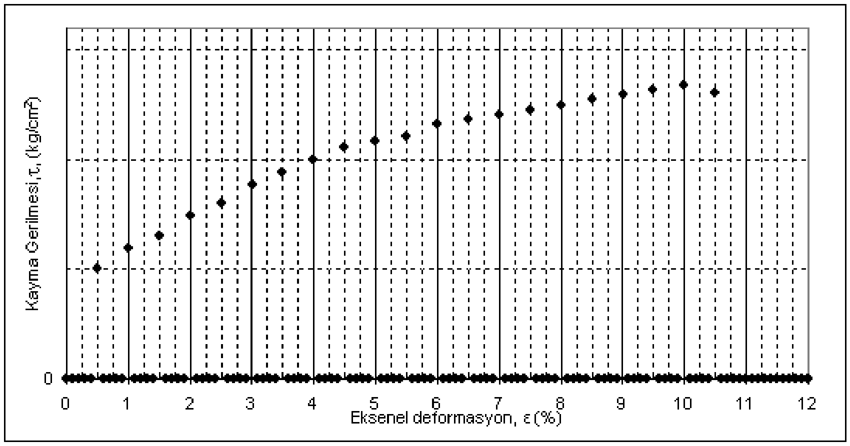

Sample no:A-1(13): $\mathbf{q_u}$ (kg/cm^2):0,67 **ΔL/L**(%):10,0.

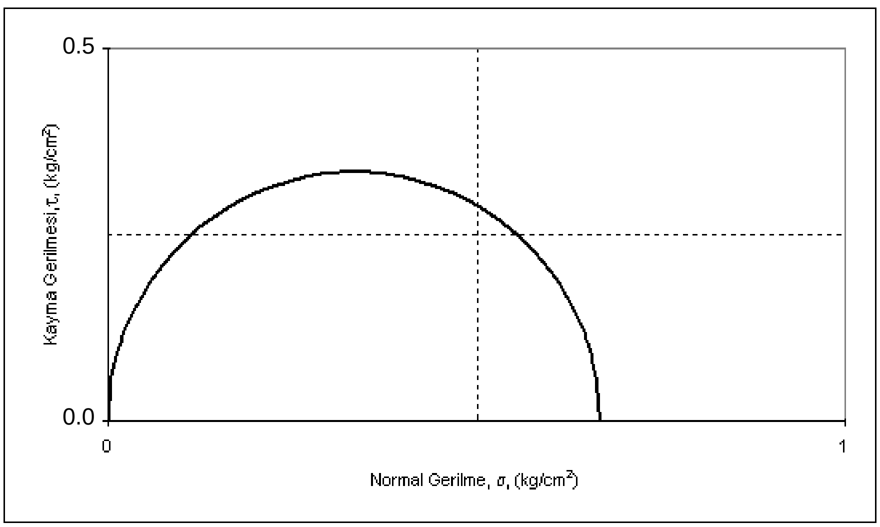

A (cm^2): 21,817 **F** (kg): 14,6.

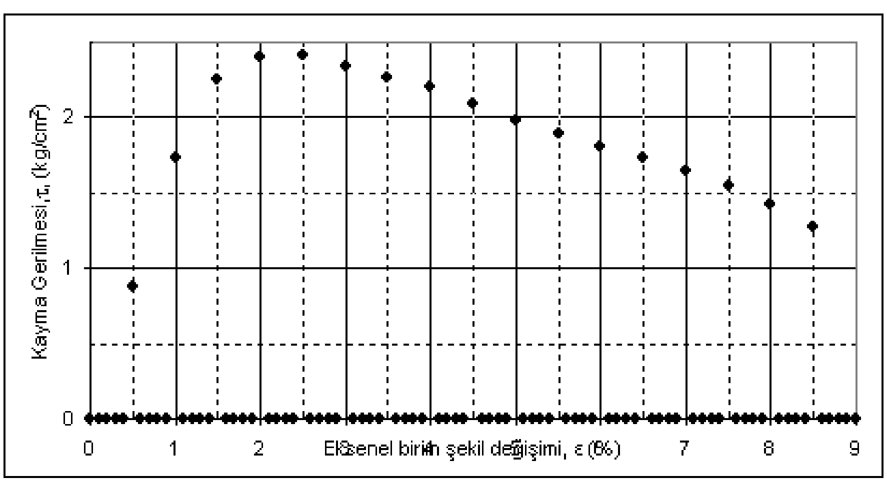

Sample no:A-1(14): $\mathbf{q_u}$ (kg/cm^2):2,42 **ΔL/L**(%):2,5.

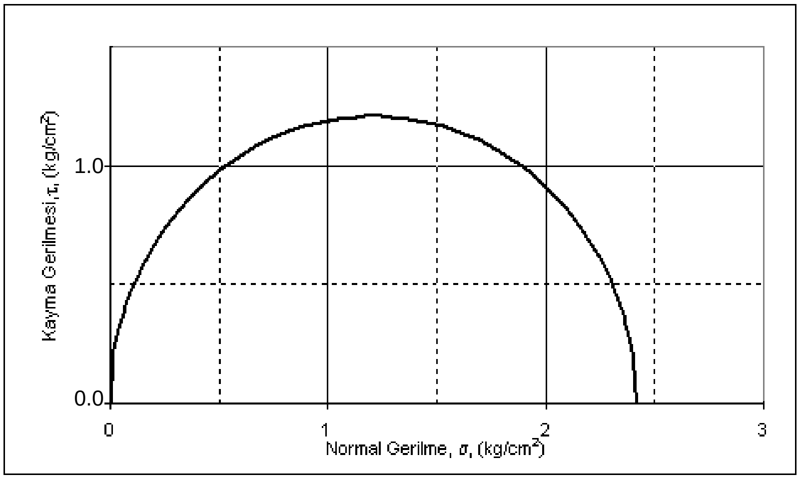

A (cm^2): 20,138 **F** (kg): 48,7.

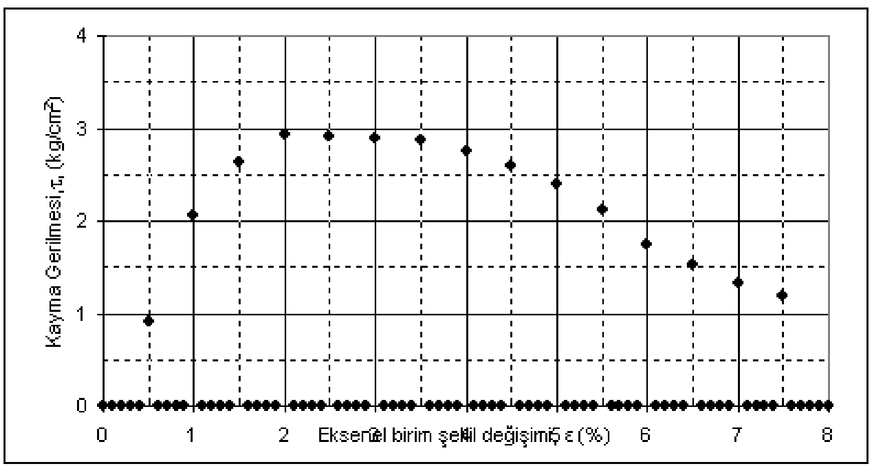

Sample no:A-1(15): $\mathbf{q_u}$ (kg/cm^2):2,92 **ΔL/L**(%):2,0.

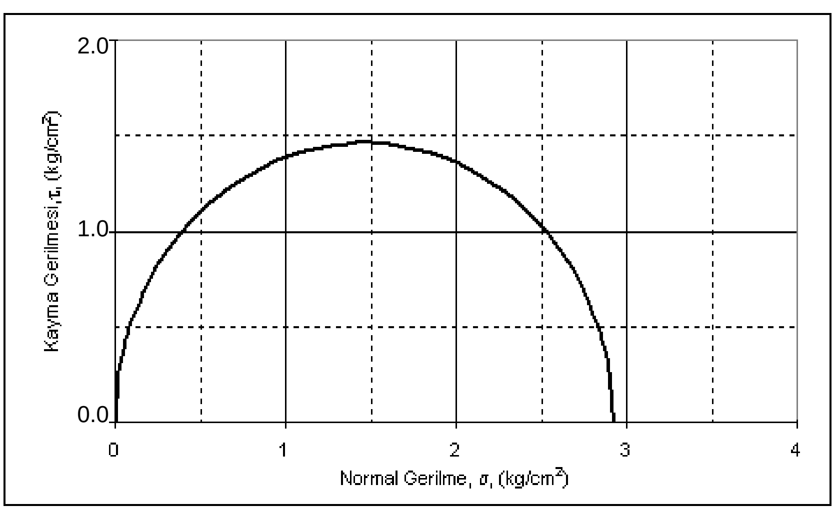

A (cm^2): 20,036 **F** (kg): 58,6.

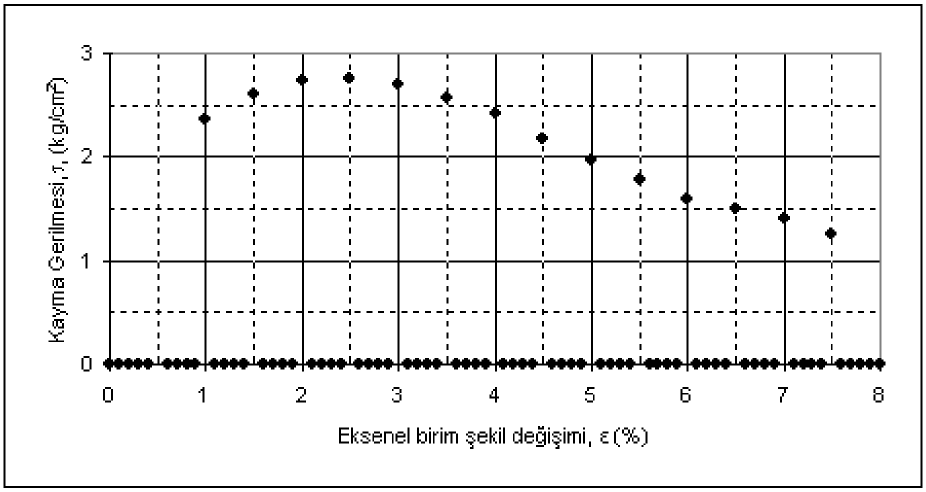

Sample no:A-1(16): q_u (kg/cm^2):3,09 **ΔL/L**(%):0,5.

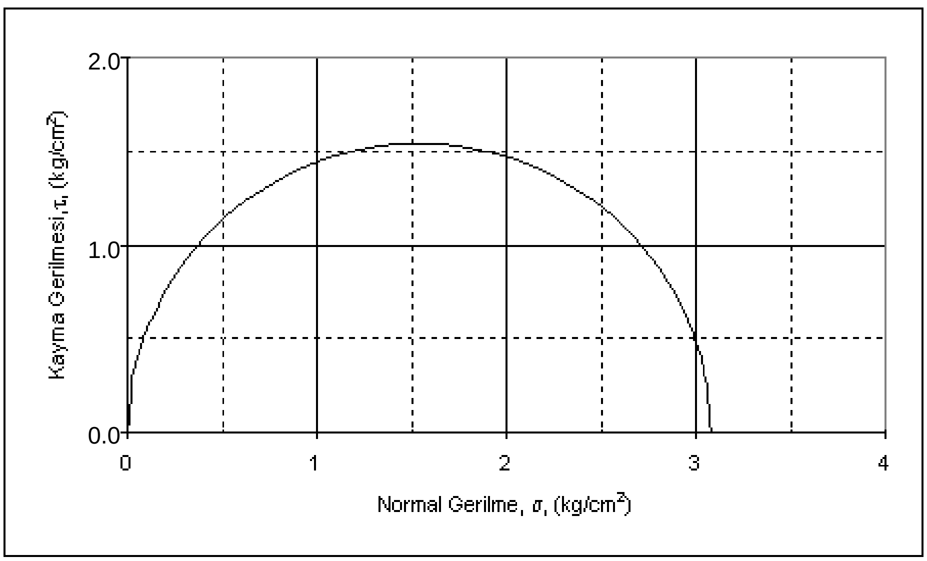

A (cm^2): 19,734 **F** (kg): 60,8.